MORPHOLOGY, SEDIMENTOLOGY AND OSL CHRONOLOGY OF THE LOWER PROSNA RIVER SYSTEM EVOLUTION – A CASE STUDY IN ROKUTÓW, WEST-CENTRAL POLAND

ANDRZEJ WOJTALAK[1,*], ROBERT J. SOKOŁOWSKI[2], PIOTR MOSKA[1]

[1]Institute of Physics, Centre for Science and Education, Silesian University of Technology, Division of Geochronology
and Environmental Isotopes,Gliwice, Poland
[2]Department of Geophysics, Faculty of Oceanography and Geography, University of Gdansk, Poland

Abstract

This paper presents comprehensive investigations of the morphological, sedimentological, and stratigraphic features in the lower Prosna River valley infill, situated in west-central Poland. At the Rokutów site, we identified two meander generations and an anastomosing system. Fluvial changes observed depict the response of the extraglacial river system to climate fluctuations post-last glaciation. Following valley aggradation, scouring erosion, reaching depths of 9–10 m, likely occurred during the Bølling Interstadial. 'Great meanders' emerged during the Allerød-Younger Dryas, persisting for around 1000 years, with an uncommon upstream rotation influenced by the sub-Quaternary surface slope. A lengthy stabilization phase, lasting 8000–10,000 years, characterized by an anastomosing system with gradual aggradation, followed the great meandering period. About 3600–3900 years ago, the valley shifted back to a fluvial system with small meanders, lasting 600–900 years. Subsequently, the River Prosna reverted to an anastomosing system, remaining so until the 19th–20th centuries when it transformed into a single-channel system through regulatory manipulation. Our research suggests that the evolution of the Prosna River differed from other rivers across Western and Central Europe, exhibiting a blend of anastomosing and meandering phases.

Keywords
lateral erosion, great meanders, fining-upward succession, GIS analysis, DEM model

1. Introduction

Fluvial systems represent one of the most widespread sedimentary environments on Earth, spanning diverse climatic zones (Bridge and Demicco, 2008; Miall, 2014). The evolution of rivers is intricately tied to factors such as base-level changes and climate fluctuations (Blum and Tornqvist, 2000). In the Late Pleistocene in Poland, the north-westward flow of rivers mitigated the impact of eustatic sea-level changes, placing greater significance on climate variations and transgressions of the Scandinavian Ice Sheet (SIS) in shaping river systems (Starkel *et al.*, 2015).

The response of lowland fluvial systems to climate shifts is evident in discernible erosion-aggradation cycles observed across numerous sites (Kozarski *et al.*, 1988; Busschers *et al.*, 2005; Vandenberghe, 2008). Within the glacial zone, successive SIS transgressions interrupted the development of fluvial systems, while in the extraglacial

zone, fluvial processes exhibited greater continuity (Peeters *et al*., 2016; Zieliński *et al*., 2019; Sokołowski *et al*., 2021). Fluvial systems in the extraglacial zone serve as valuable archives of climate changes, offering opportunities for the detection and reconstruction of palaeoenvironmental changes and the construction of time-climate models through multi-proxy studies (Gabris and Nador, 2007; Gębica *et al*., 2015; Panin and Matlakhova, 2015).

A pivotal period of climate change occurred during the decline of the last glaciation, resulting in a fundamental shift in the sedimentation style of river systems in the European Lowlands from braided to meandering sedimentation style. This transformation transpired during the transition from the Late Pleniglacial to the Bølling Interstadial (Vandenberghe *et al*., 1994; Mol *et al*., 2000; Vandenbeghe and Sidorchuk, 2020). Subsequent developments in fluvial processes during the Holocene led to the formation of smaller meanders, characterised by well-preserved organic sediments within cut-off palaeo-meanders (Kasse *et al*., 2010).

The Prosna River, an extraglacial river in the Polish Lowlands and a left-bank tributary of the Warta River in western Poland (**Fig. 1A**), showcases pronounced large meanders from the Late Glacial period alongside generally Holocene-age smaller meanders, as described in the lower Prosna River valley (Rotnicki, 1987). This intricate network of palaeo-meanders offers a unique opportunity to study in detail various critical aspects of fluvial processes and to pinpoint the chronological evolution of these features. To address this, we selected a palaeo-meander near the Rokutów village as a case study (**Figs. 1B,C**). This specific meander was chosen for its well-preserved depositional forms from two distinct phases of meandering processes, as observed along the present-day Prosna River channel in the cut-bank of the river. Our research objectives include as follows: (i) determining the morphology of these meanders; (ii) reconstructing depositional processes; and (iii) establishing the timeframe of meander formation processes based on optically stimulated luminescence (OSL) dating.

2. Regional Setting

The study site is situated along the left bank of the Lower Prosna River valley in the eastern section of the Wielkopolska region, western Poland (**Fig. 1A**). During the one before last glaciation (the Warta glaciation, final part of the Marine Isotope Stage 6a) the area was covered with the SIS. Positioned approximately 20 km southeast of the Last Glacial Maximum (LGM), as established by Rotnicki and Borówka (1990) and Marks *et al*. (2016), the study site reveals a rich geological history and at least four

fluvial terraces formed after Marine Isotope Stage (MIS) 6a glaciation (**Figs. 1B,D**). Beneath the Quaternary series, the presence of Upper Miocene clays is evident (**Fig. 1E**). The Quaternary deposits within the Lower Prosna River valley exhibit varying thickness, ranging from 2–3 m to 12–18 m, as reported by Szałamacha (1999) and Rotnicki *et al*. (2005). The higher Prosna River terraces primarily consist of glacial till, directly overlaying Miocene clays. This till, deposited during the Late Saalian (Marine Isotope Stage 6a) SIS transgression, is succeeded by glaciofluvial sands and gravels, reaching thicknesses of 5–7 m (**Fig. 1D**). The deposition of this series occurred during the recession phase of the Late Saalian glaciation. The investigated fluvial deposits lie approximately 8.5 m below the upper terrace (**Fig. 1D**).

The formation of the Prosna River valley occurred in several phases. The initial phase develops during the concluding stages of the Warta glaciation (Marine Isotope Stage 6a), marked by the southward flow of melt-out water during deglaciation (Szałamacha, 1999). The second phase transpired during the Eemian interglacial, characterised by a northward flow direction (Rotnicki, 1987). In the Weichselian glaciation (*sensu lato*), six terraces were formed (Rotnicki and Borówka, 1990). Throughout the last glaciation, the Prosna River valley functioned as an extraglacial river, serving as a tributary to the pre-Warta river system. The Prosna River mouth, situated approximately 20–30 km to the north, fell within the direct influence of the LGM extent. In the latter part of the Late Pleniglacial, a braided-river system prevailed, accompanied by aggradation of sandy series within the valley. The transition from a braided to a meandering system likely occurred at the onset of the Late Glacial period (Kozarski *et al*., 1988). During the Late Glacial period, heightened river incision and the formation of sandy terraces and large meanders facilitated the intensification of aeolian processes, giving rise to inland dunes with palaeosols (Moska *et al*., 2022, 2023). Throughout the entire Holocene, the lower segment of the Prosna River operated within a meandering system, contributing to the formation of at least two generations of meanders (Rotnicki and Borówka, 1990).

3. Materials and Methods

Thorough investigations were conducted at two distinct exposures. The initial exposure was situated in the northwestern section of the expansive meander, delving to a depth of 1.6 m (**Fig. 2**). Material for the survey was meticulously collected from a depth of 0.5 m below the groundwater level, using a steel pipe for extraction and secure handling. The second exposure was situated in the erosional undercut of the Prosna River within the confines
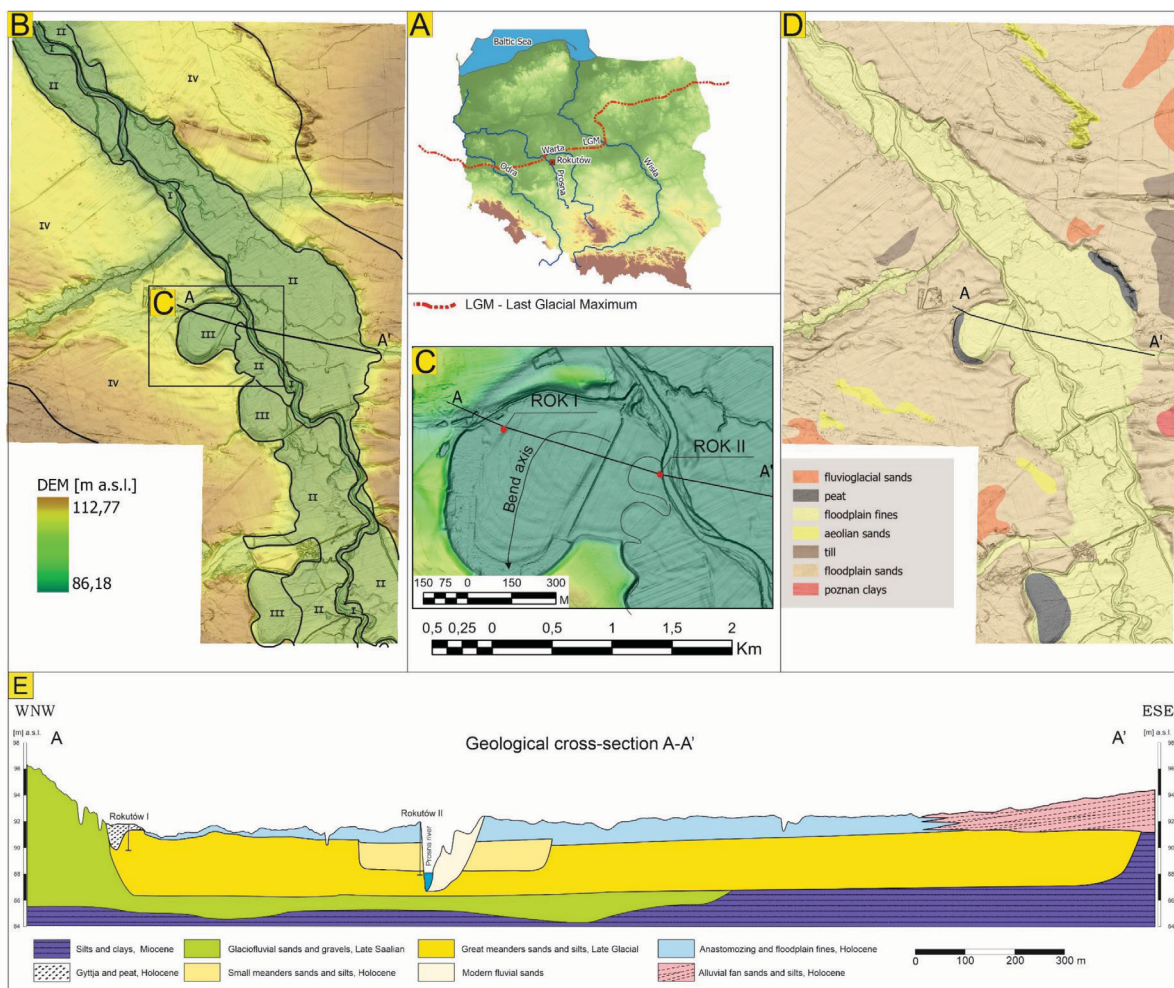
Fig 1. *A – Location of study area on the map of Poland; B – DEM with fluvial terraces; C – Detail DEM of the study area with location of studied profiles; D – Generalised geological map (after – Szałamacha 1999), modified. E – Geological cross-section through the Prosna Valley. DEM, Digital Elevation Model.*

of a smaller meander. In this instance, sediments with a depth of up to 4.5 m were meticulously analysed across an approximately 30 m width. Sediment samples were gathered from both exposures, laying the groundwork for subsequent laboratory studies.

3.1. GIS Analysis

The Geological Information System (GIS) analysis was conducted using a digital elevation model (DEM), specifically a raster data type generated from asc extension files. These files are essentially text files that construct a raster matrix separated by spaces. The analysis focused on the Prosna River valley segment stretching from Budzynek to Bogusław (**Fig. 1B**), with GIS data sourced from the open-access platform www.geoportal.gov.pl. The initial horizontal resolution of the raster data was 1×1 m, but resampling to a 2×2 m resolution was executed to eliminate fine-scale

disturbances like ploughing marks in the fields. The raster data underwent processing through the Topographic Position Index (Weiss, 2001; Newman *et al*., 2018), with the results used to generate the relief maps in **Figs. 1 and 2**. Various geospatial functions were applied in the GIS analyses, including resampling, aggregation, calculation of flow direction and flow accumulation, slope and DEM no sinks. These geostatistical operations were crucial for calculating the Topographic Wetness Index (TWI, Sørensen *et al*., 2006), employed to delineate the spatial extent of meanders. The GIS analysis proved instrumental in pinpointing the locations of documentary sites within the Prosna River valley study area. The study identified four separate river terraces, detailing their altitude and fluvial characteristics (**Fig. 1B**). Furthermore, for the great meander at the Rokutów site, the number, length, height and width of scroll bars were precisely determined (Przedwojski, 2006).
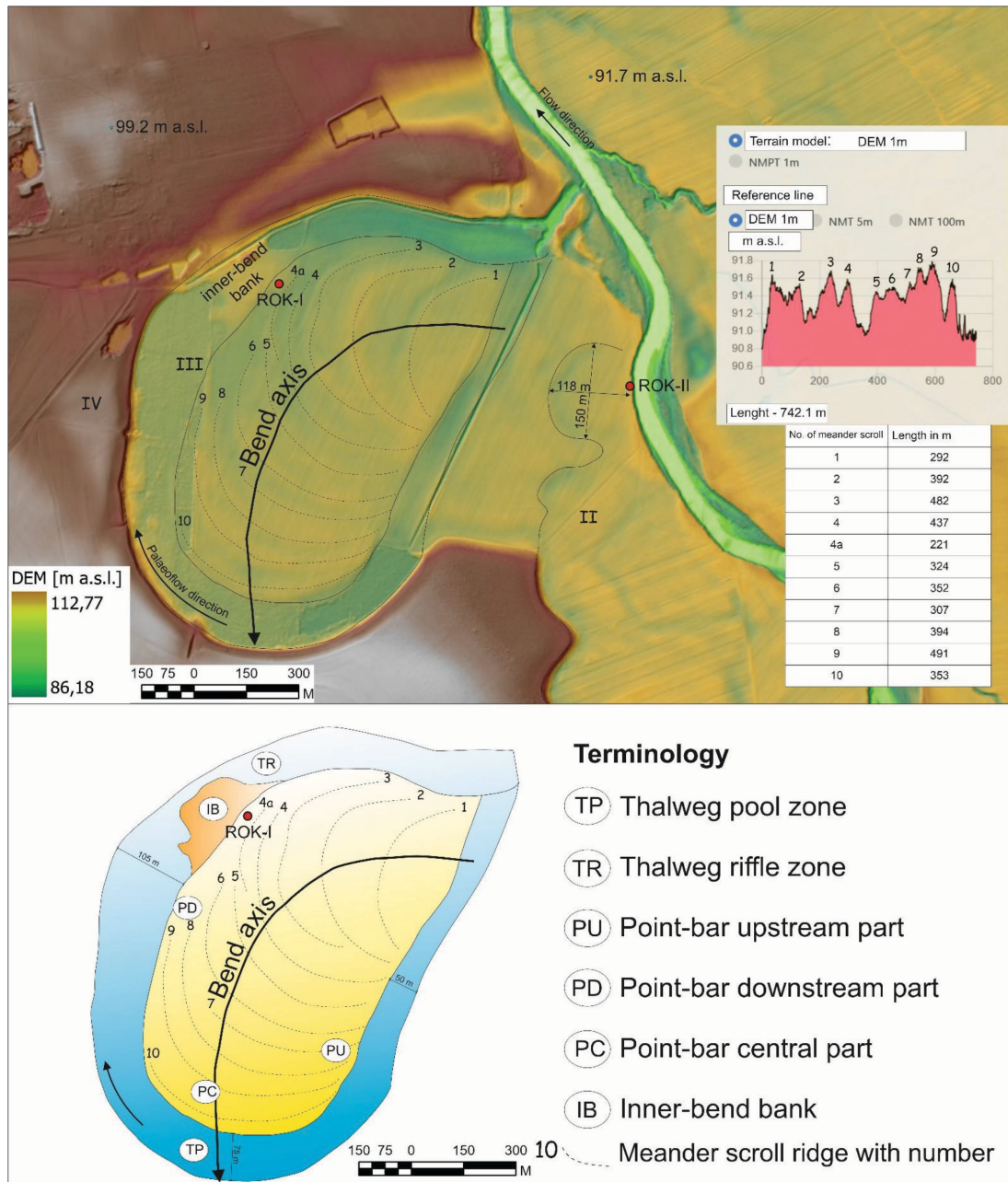
Fig 2. *Morphology and morphometry of the great meander in the Rokutów site. Terminology of meandering elements after Ghinassi et al. (2014), modified.*

3.2. Lithofacial Analysis

A comprehensive lithofacial analysis was conducted to reconstruct sedimentary processes and their chronological sequence, with the outcomes presented in **Figs. 3 and 4**. Structural aspects such as size, shape, stratification or lamination, along with textural considerations like grain-size distribution, were systematically examined to identify lithofacies types. The analysis adhered to the methodology proposed by Miall (1978, 2006) and incorporated additional recommendations by Zieliński (2014). Nineteen samples were meticulously collected from both profiles for granulometric analysis, as illustrated in **Fig. 3**. Approximately 400 g of sediment sample was utilised for this analysis. The results were used to generate grain-size
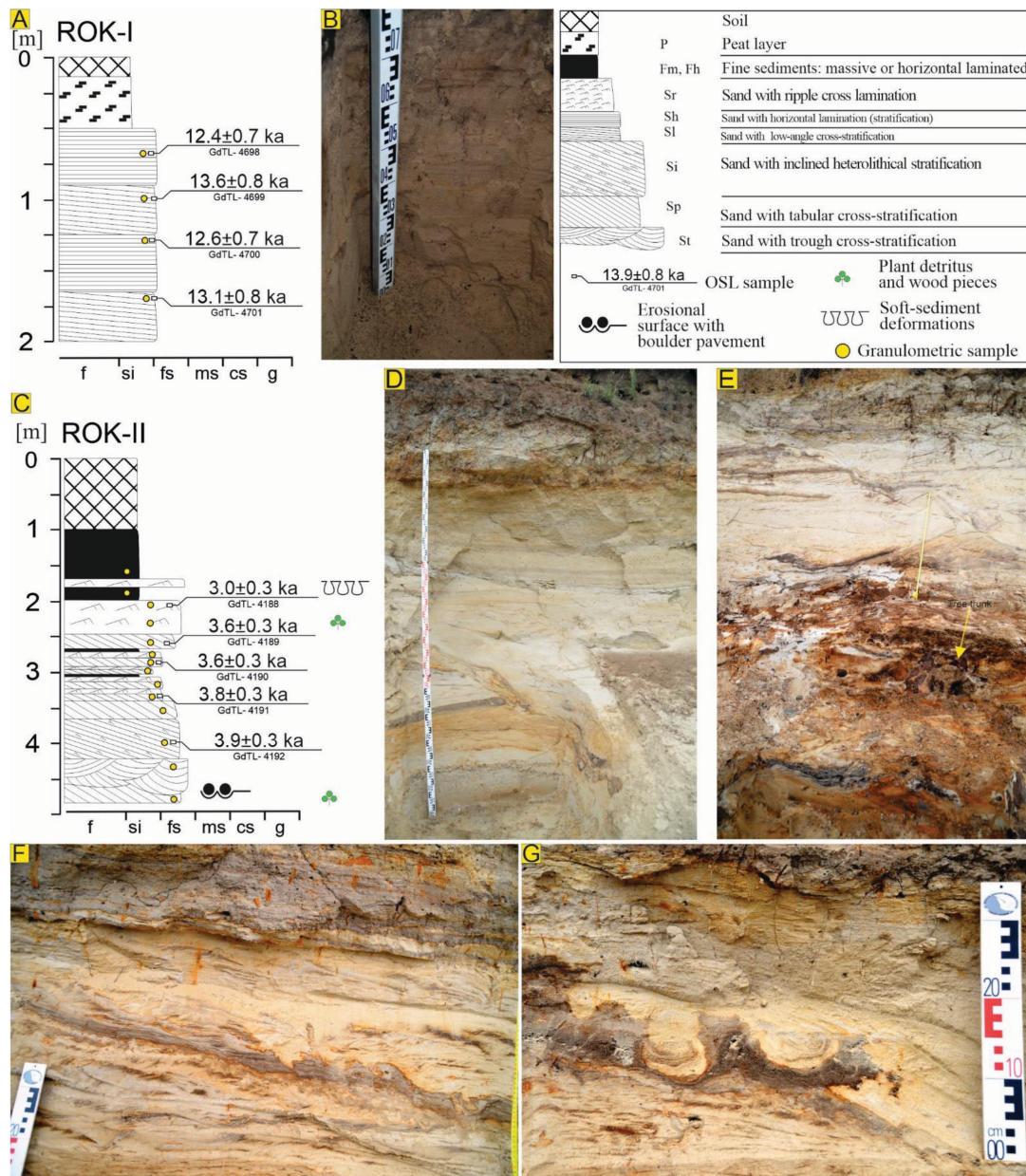
Fig 3. *A – Profile ROK-I; B – Stratified sands in the ROK-I profile; C – Profile ROK-II; D – Fining-upward succession of the point bar with erosional channel in the central part; E – Lower part of the point-bar succession with tree trunks (yellow arrow) in the lower part of the point bar; F – Transition of upper part of the point bar (sands with ripple cross-lamination) into fine sediments of the floodplain; G – SSDs in the upper part of the point bar. SSDs, soft-sediment deformations.*

curves on a logarithmic scale, and subsequent statistical parameters – including mean diameter, sorting, kurtosis and standard deviation (skewness) – were calculated, as present in **Fig. 4** (Rząsa and Owczarzak, 2013). The granulometric analysis was processed using the methodology outlined by Folk and Ward (1957) and implemented through the Gradistat software.

3.3. OSL Dating

Four samples from the ROK-I profile and five from the ROK-II were taken for OSL dating (**Fig. 3**). Samples from the ROK-I profile were collected from upper part of the point-bar succession (lithofacies *Si*). In the ROK-II profile samples were taken from all main parts of the point-bar succession and different lithofacies (**Fig. 3**). The measurements
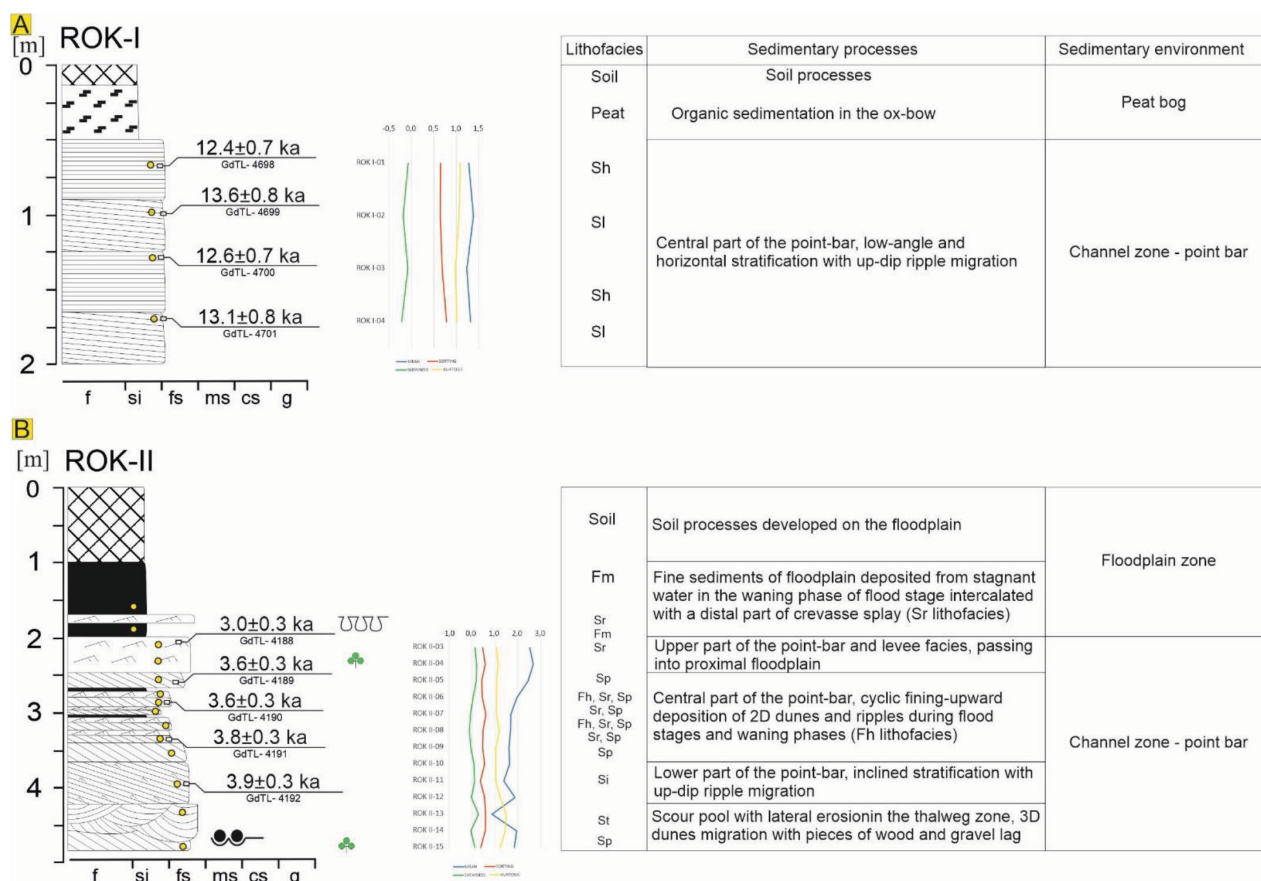
Fig 4. A,B – Profiles with results of grain-size analysis and interpretation of sedimentary processes and environments.

have been carried out in the Gliwice luminescence dating laboratory (Moska *et al*., 2021). For dose rate determination high-resolution gamma spectrometry using an HPGe detector manufactured in Canberra was used in order to determine the content of U, Th and K in the sample according to the laboratory protocol (Moska *et al*., 2021). Dose rates were calculated using online dose rate calculator (Tudyka *et al*., 2023), which contains all the latest conversion factors. We assumed that the average water content was $15 \pm 3\%$. All necessary data for dose rate calculations are presented in **Table 1 and Fig. 5**. For OSL measurements, coarse grains of quartz (125–200 μm) were extracted from the sediment samples by routine treatment with 20% hydrochloric acid (HCl) and 20% hydrogen peroxide (H_2O_2) (Aitken, 1998).

The grains underwent a sieving process, followed by separation based on density using sodium polytungstate solutions, resulting in grains with densities ranging from 2.62 g/cm³ to 2.75 g/cm³. Eventually, the grains underwent etching with concentrated hydrofluoric acid (HF).

All OSL measurements were performed using an automated Risø TL/OSL DA-20 reader fitted with a calibrated $^{90}Sr/^{90}Y$ beta source delivering about 6.0 Gy/min to grains at sample position and a 6 mm Hoya U-340 filter was mounted during OSL measurements. Equivalent doses were determined using the single-aliquot regenerative-dose (SAR) protocol (Murray and Wintle, 2000). Final equivalent dose (De) values were calculated for all samples using the Central Age Model (CAM) or Minimum Age Model (MAM) (Galbraith *et al*., 1999) using R package 'Luminescence' (Kreutzer *et al*., 2020). All obtained age distributions are presented in **Figs. 3,4 and Tab. 1,** where the age distribution is presented in terms of relative probability density functions (Berger, 2010). Overdispersion parameter for samples from ROK-II profile was higher than 20% with not unimodal distributions, so for those samples MAM was used. For samples from ROK-I profile series, distributions are unimodal and overdispersion parameters are much lower than 20%, therefore it can be assumed that the tested material represents a group of the well-bleached quartz (Moska, 2019) and CAM model can be applied for final equivalent dose calculation.

Table 1. All important data for investigated luminescence samples: sample names, depth, radionuclid concentration, overdispersion parameter, dose rate, equivalent dose (CAM model) and final age.

Lab.Code	Sample ID	Sampling depth (cm)	U-238 (Bq/kg)	Th-232 (Bq/kg)	K-40 (Bq/kg)	Water content (%)	Overdispersion (%)	Dose rate (Gy/ka)	Equivalent dose (Gy)	OSL age (ka)
GdTL-4188	TUR_1	210	7.8 ± 0.4	8.3 ± 0.4	234 ± 11	15 ± 5	22	1.18 ± 0.04	3.25 ± 0.26	2.75 ± 0.24
GdTL-4189	TUR_2	260	8.9 ± 0.4	10.0 ± 0.5	181 ± 9	15 ± 5	24	1.06 ± 0.04	3.43 ± 0.28	3.23 ± 0.27
GdTL-4190	TUR_3	280	5.1 ± 0.3	5.6 ± 0.3	149 ± 7	15 ± 5	32	0.83 ± 0.04	2.62 ± 0.26	3.16 ± 0.29
GdTL-4191	TUR_4	340	4.4 ± 0.3	3.8 ± 0.3	148 ± 7	15 ± 5	30	0.77 ± 0.04	2.58 ± 0.25	3.35 ± 0.32
GdTL-4192	TUR_5	410	5.1 ± 0.3	5.9 ± 0.3	143 ± 7	20 ± 5	25	0.79 ± 0.04	2.63 ± 0.24	3.32 ± 0.32
GdTL-4698	ROK_1	70	4.1 ± 0.2	3.3 ± 0.3	126 ± 10	15 ± 5	5	0.67 ± 0.03	8.1 ± 0.2	11.9 ± 0.6
GdTL-4699	ROK_2	100	3.0 ± 0.2	3.1 ± 0.3	113 ± 9	15 ± 5	11	0.61 ± 0.03	8.0 ± 0.3	13.1 ± 0.8
GdTL-4700	ROK_3	125	3.6 ± 0.2	3.0 ± 0.5	128 ± 10	15 ± 5	10	0.65 ± 0.03	8.0 ± 0.2	12.2 ± 0.7
GdTL-4701	ROK_4	160	4.5 ± 0.2	3.4 ± 0.3	131 ± 10	20 ± 5	10	0.63 ± 0.03	8.3 ± 0.3	13.1 ± 0.8

CAM, Central Age Model; OSL, optically stimulated luminescence.

4. Results

4.1. Morphology

Based on the analysis of the DEM, we identified four distinct river terraces (**Fig. 1B**). The highest terrace (IV) is situated at an elevation of 98–97 m above sea level (a.s.l.) and is thought to represent the Late Pleniglacial phase of fluvial aggradation. Terraces III and II were delineated due to visible river incision, leading to the formation of a meandering system. Terrace III, positioned at an elevation of 91.5–91.0 m a.s.l., comprises what are referred to as large meanders. These meanders exhibit a diameter following meander accretion of 742 m, with a perpendicular dimension of 495 m (**Fig. 2**). The difference in elevation between the oxbow infill surface and the culminations of point-bars does not surpass 1.8 m. The large meander is characterised by 10 scroll bars (swale and ridge pairs) spanning the entire width of the meander, along with one shorter scroll (scroll No. 4a, **Fig. 2**). The lengths of the scroll bars range from 221 m to 491 m, with individual heights not exceeding 0.7 m. The point bar axis extends for 742 m (**Fig. 2**), altering its trajectory from an initial westward orientation to a southern direction. Interestingly, this change is in direct contrast to the primary outflow direction in the valley (North - West).

Terrace II is situated at an elevation of 91.0 m a.s.l. and features a small-meander system along with sinusoidal channels characteristic of an anastomosing system. The observed second meander spans a length of 118 m and a width of 150 m. Remarkably, it exhibits no discernible signs of rotation or translation. Unfortunately, potential scroll bars within this meander are concealed beneath a thicker layer of floodplain sediments, measuring up to 2 m in veils indepth. Consequently, the morphology lacks distinguishable and measurable meander scrolls. Located at the base of this meander, within the Prosna River undercut, is the ROK-II profile. Terrace I, recognised as a flood terrace, is believed to have formed in the Late Holocene and has been influenced by human activities. It is positioned at an altitude of 90 m a.s.l.

4.2. Sedimentary Succession

The examined profiles showcase two distinct generations of meander formation. The ROK-I profile unveils an older and more expansive meander, while the ROK-II profile exposes a sequence associated with a younger and more compact meander.

The cumulative thickness of sediments in the ROK-I profile measures 2 m (**Fig. 3A**). These sediments are characterised by medium-grain sands exhibiting low-angle and horizontal stratification (**Fig. 3B**). The analysed sediments display homogeneity in grain size (**Fig. 4A**). Immediately above the sands, a 0.5 m thick layer of peat is present, which has undergone transformation due to agrotechnical
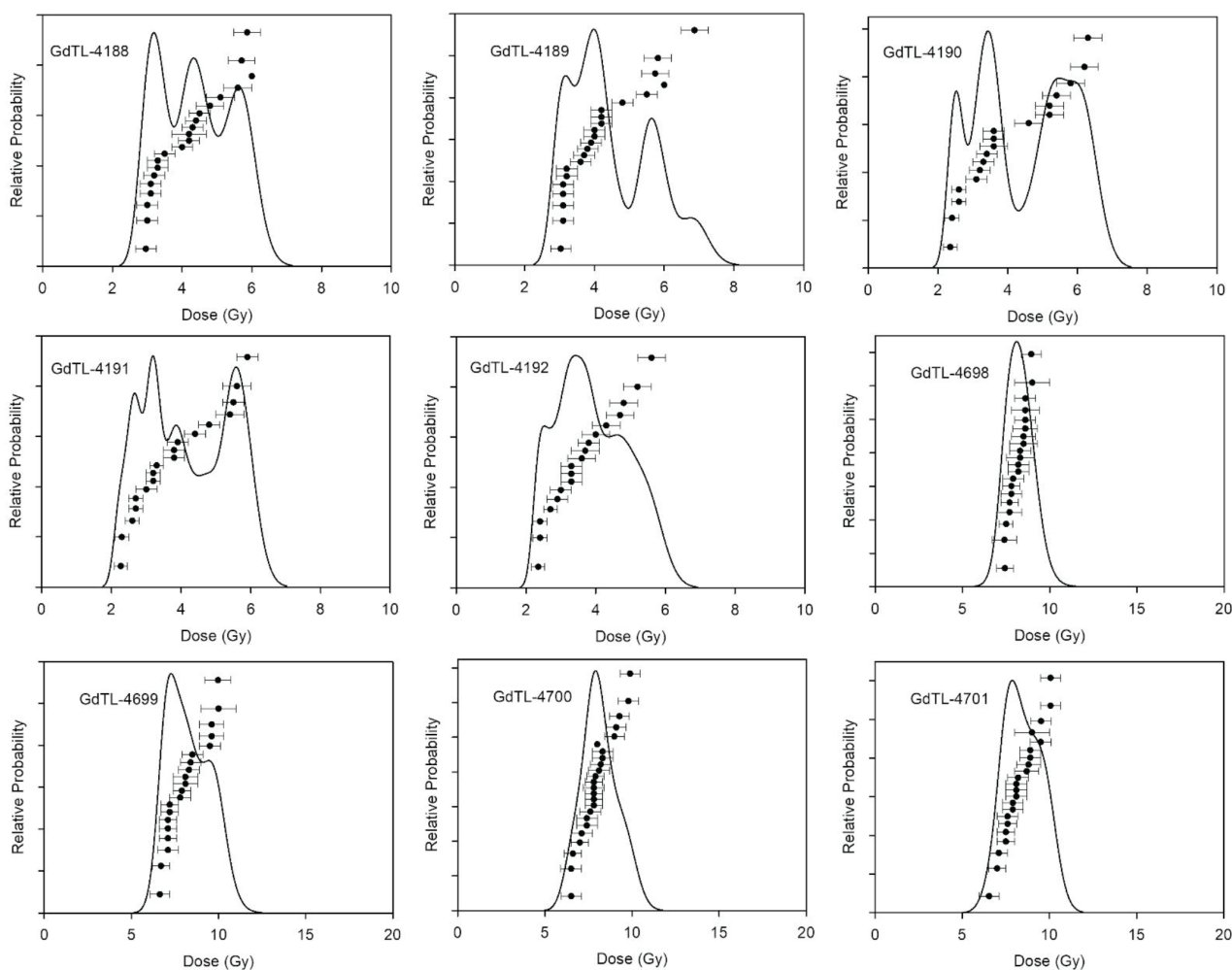
Fig 5. Dose distributions for all tested samples.

processes. This sandy peat, cultivated for agriculture, is adorned with the roots of contemporary plants and, consequently, has not been sampled for radiocarbon dating.

The sedimentary sequence in the ROK-II profile reaches an impressive thickness of nearly 5 m (**Fig. 3C**). This sequence follows a fining-upward (**Fig. 3D**). Towards the lowermost section of the profile, a prominent erosional surface is observed. Just above it, there is a layer of mid-grained sand with fine gravels and fragments of tree trunks exhibiting a massive to through-stratified structure (**Fig. 3E**). Progressing upward, the sediments transition from medium-grained sands with planar cross-stratification to fine-grained sands featuring ripple cross-lamination. Within the central portion of the profile, an erosional channel is discernible, filled with inclined cross-stratification and displaying ripple marks in its upper segment. Above the channel infill, fine-grained sands with ripple cross-lamination gradually transform into silty sands containing dispersed plant detritus (**Fig. 3F**). Notably, these lithofacies exhibit small

soft-sediment deformations (SSD) with thicknesses of up to 10 cm. The uppermost segment of the profile comprises silts and organic muds interspersed with sandy strings forming ripples, showcasing both horizontal and massive structures (**Fig. 3G**).

4.3. OSL Dating Results

Four sediment samples were collected from the ROK-I profile for age dating using the OSL method. The obtained dating results span from 13.6 ± 0.8 ka (GdTL-4701) to 12.4 ± 0.7 ka (GdTL-4698) in the upper segment of the profile (**Table 1 and Fig. 5**). These results strongly suggest that sediment deposition occurred within the timeframe of 13.5–12.5 ka.

In the case of the ROK-II profile, OSL dating results ranging from 3.9 ± 0.4 ka (GdTL-4192) in the lower portion to 3.0 ± 0.3 ka (GdTL-4188) in the upper section (**Fig. 3C**). Remarkably, the temporal span of depositional processes did not exceed 1000 years.

5. Discussion

Through morphometric and morphological analysis, we successfully distinguish two distinct generations of meanders. These findings find reinforcement in OSL dating and lithological features, notably preserving shared characteristics of meander point bars such as lateral accretion perpendicular to the valley axis, fining-upward profiles and the prevalence of overbank and ox-bow facies at the summit (Ghazi and Mountney, 2009; Ghinassi et al., 2014).

5.1. Sedimentary Processes

The progradation of the great meander in the Rokutow site indicates its upstream rotation with a contraction (Lin et al., 2021). This is rather uncommon, given that meanders typically exhibit expansion perpendicular to the valley axis or downstream translation with rotation, as noted by Ghinassi et al. (2014). The distinctive rotation and contraction in this instance may be attributed to the relatively narrow valley in comparison to the meander radius and the specific lithology of the substrate (**Fig. 1E**). This challenging scenario may have arisen due to difficulties in eroding in a direction consistent with the valley gradient, a phenomenon well-documented by Nanson and Hickin (1986) and Parker and Andrews (1986). The resistant Miocene clays, positioned at depths ranging from a few to several meters beneath the ground surface (as indicated by Szałamacha, 1999), served as the resistant substrate in this context. It is presumed that the meander effectively 'slid' down the inclined surface of the Miocene clays, moving in a direction almost opposite to the valley gradient. Further studies involving an in-depth examination of other large meanders in the Lower Prosna valley, combined with a comprehensive survey of their respective substrates, will help substantiate this hypothesis.

The prevalence of medium-grained sands in the examined outcrop within the expansive meander unveils insights into two key factors: the fraction of available material sourced from the eroded outer bank and the energetic dynamics of the river stream. Due to elevated groundwater levels, excavation of the outcrop to a greater depth was impossible. Nonetheless, it is reasonable to infer that the average grain size is larger than what is typical in fining-upward point bar profiles (as outlined by Galloway and Hobday, 1996; Miall, 2006). This suggests a predominant sandy fraction, resulting in an estimated potential specific stream power (ωpv) of approximately 10^1 W/m^2 (according to Kleinhans and van den Berg, 2011). The channel width exhibited variations, ranging from 50 m in the upstream section to 105 m in the downstream section, with a central section width of 75 m (**Fig. 2**). The presumed depth of the channel at full-bank discharge reached approximately 6 m (**Fig. 1E**). In comparison, the average width of the contemporary Prosna channel in the study area is around 25 m,

while the channel depth in the meander apex reaches 3–4 m. This allows us to assume that, as with other rivers of the European Lowlands, the flows in the Prosna River in the Late Glacial were clearly higher than modern flows.

The subsequent generation of meanders, as examined in the ROK-II section, is positioned at the same altitude as the older meander (**Fig. 1**). This suggests that the Holocene erosion in this segment of the Prosna River valley was predominantly of the lateral type, setting it apart from other rivers in the Polish Lowlands (as noted by Kozarski et al., 1988; Pożaryski and Kalicki, 1995). The analysed profile provides a full succession of the laterally migrating point bar (**Fig. 4B**), with the overall sediment thickness indicating that the full channel flow reached depths of around 4 m. The lower boundary is characterised by an erosional type, evident in the gravel lag and tree trunk pieces (**Fig. 3E**). The presence of numerous crystalline rocks in the gravel-sized material, originating from Scandinavian area (primarily from the SIS), suggests reworking during post-Saalian fluvial processes (Rotnicki, 1987). The preserved shape of the meander indicates a straightforward expansion perpendicular to the main valley axis (Ghinassi et al., 2014). The size of the meander, particularly the width of the palaeochannel (20 m), closely mirrors that of the present-day Prosna River, implying a relatively consistent fluvial regime. The mean grain size reveals a fining-upward (**Fig. 4B**). Thick overbank deposits (up to 2 m) in the upper section of the profile were deposited during frequent flood episodes in the Upper Holocene, followed by the sedimentation of fine material with dispersed organics. Small SSDs observed in the upper part of the point bar (**Fig. 3G**) formed due to rapid deposition on the slope of the outwash, influenced by frequent changes in the river water level and partial liquefaction of the deformed sediments (Pisarska-Jamroży and Weckwerth, 2013). Considering the large thickness of overbank sediments, the lower Prosna valley displayed a general trend of slow aggradation during the Late Glacial and Holocene, primarily of fine sediments. Notably smaller Holocene meanders, comparable to those in other river systems of the European Lowlands, are interpreted as a consequence of reduced discharge in the Holocene compared with the Late Glacial (Vandenbrghe et al., 1994; Rotnicki and Młynarczyk, 1998; Vandenberghe, 2015). The 4-m deep incision of the Prosna River occurred after 2 kyr ago and is presumed to be associated with historical times and human regulation of the river (Małecki and Ptak, 2015). Further exploration beyond the scope of this article is required to delve into this aspect.

5.2. Chronology of Fluvial Processes

The genesis of the first generation of meanders took place during the Late Glacial period. OSL dating results point to their formation occurring in the Allerød, extending
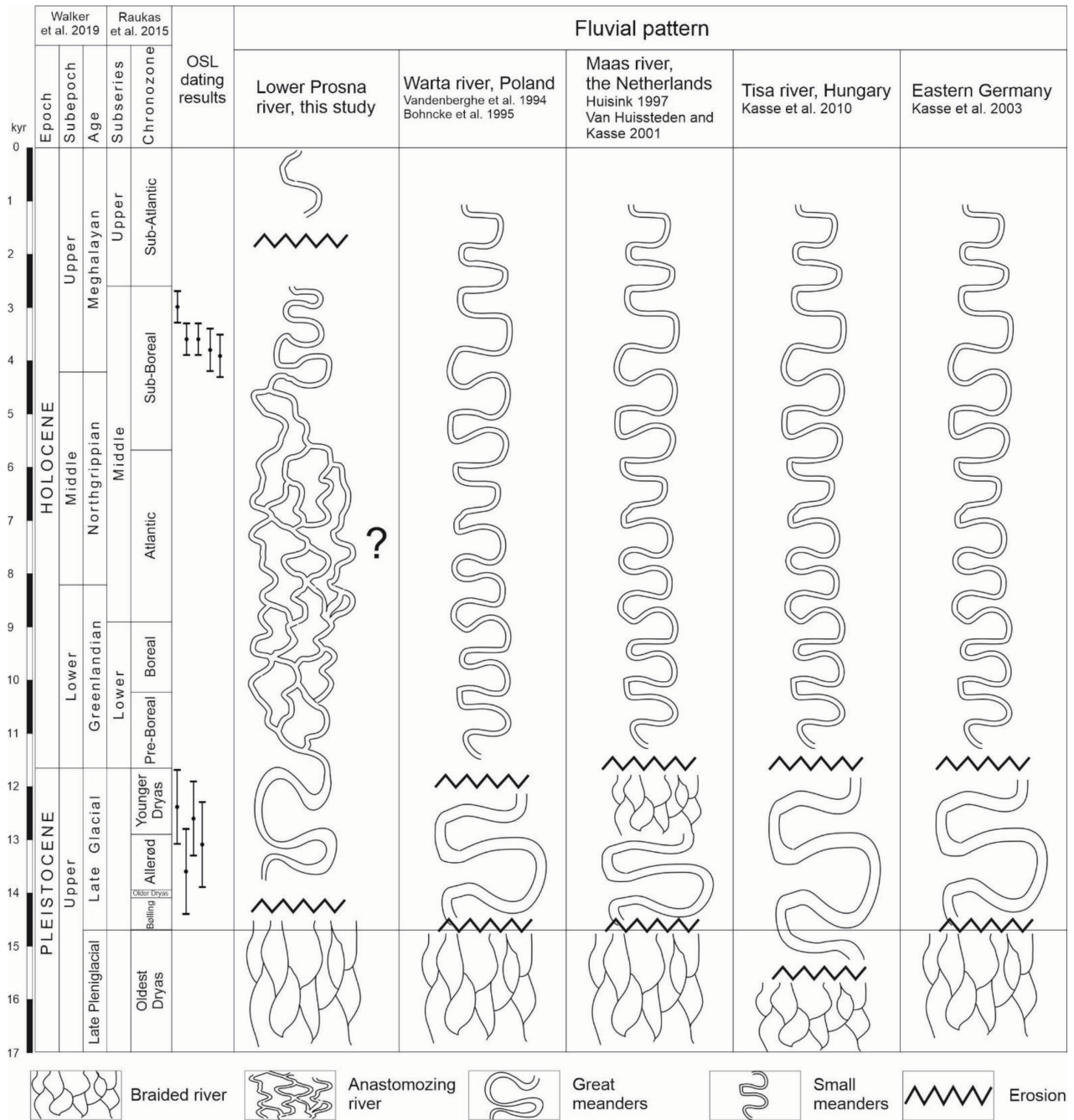
Fig 6. *Synthesis of fluvial system changes of the lower Prosna River (this study, Poland), Warta River (Poland, Vandenberghe et al., 1994; Bohncke et al., 1995), Maas River (the Netherlands, Huisink 1997; Van Huissteden and Kasse 2001), Tisa River (Hungary, Kasse et al., 2010) and Eastern Germany (Kasse et al., 2003).*

possibly into the Younger Dryas (**Fig. 6**). Similar conclusions on the formation of great meanders in the middle and lower sections of the Prosna River valley were previously proposed by Rotnicki and Latałowa (1986). It is important to note that our analysis specifically focused on the upper part of the point-bar succession, which is part of the great meander of terrace III. The exploration of oxbow lake infilling at the Grodzisko site, situated on the left bank of the Lower Prosna River approximately 6.5 km northwest of the Rokutów site, provides additional insights. These studies suggest that the cut-off of meanders coincided with the Younger Dryas (refer to Gałka *et al*., 2020). The

synchronicity in the timing of the formation and cutting of the great meanders is consistent across the Eastern and Central European Plains (Vandenberghe and Sidorchuk, 2020). Comparisons with larger rivers in central and western Europe, such as the Warta River in Poland, the Niers-Rhine Rivers in western Germany and the White Elster River in eastern Germany, reveal that braided channels became inactive at the outset of the Bølling and were succeeded by extensive meandering systems (as documented by Kozarski *et al*., 1988; Kozarski 1991; Mol *et al*., 2000; Kasse *et al*., 2005; Starkel *et al*., 2007). Our findings suggest that the process of great meander formation at the Rokutów site might have commenced somewhat later than observed in these larger rivers (**Fig. 6**). The potential for a differing age of large meander development is hinted at by results from the Pannonian Plain and Eastern Europe, where such meanders formed during the Late Pleniglacial (Sidorchuk *et al*., 2001; Kasse *et al*., 2010). This intriguing issue warrants further investigation, particularly focusing on the primary segment of the large meander at the Rokutów site.

In the European Lowlands region, following the formation of great meanders, fluvial processes develop in diverse scenarios (**Fig. 6**). In western Europe, the development of great meanders ceased due to pronounced climate deterioration during the Younger Dryas, leading to the resurgence of a braided style of fluvial processes (as documented by Vandenberghe *et al*., 1994; Kasse *et al*., 2005). Conversely, in central and eastern Europe, as well as in the Pannonian Plain, a shift to a braided river did not occur during the Younger Dryas (see Kozarski *et al*., 1988; Sidorchuk *et al*., 2009; Kasse *et al*., 2010). During the Early Holocene, the size of meanders underwent reduction due to changes in the hydrological regime, with smaller meanders becoming predominant and the formation of several river terraces (see Kozarski, 1991). In the Lower Prosna River valley, the post-formation history of fluvial processes following the great meanders of the Late Glacial period appears to exhibit a slightly different pattern. The analysis of the DEM of terrace II suggests the possibility of an anabranching/anastomosing style of fluvial processes (**Fig. 6**). This is evident in the network of small, sinuous channels dissected by minor meanders. Notably, all morphological elements in the study area are situated at the same altitude, without apparent traces of river incision post the formation of great meanders (**Fig. 1B**). The assumed anastomosing phase is presumed to have occurred during the Lower and Middle Holocene, facilitated by the relatively low gradient of the river (averaging 0.82‰, according to Kaniecki, 1976). However, the absence of dating results

from these sediments limits stratigraphic verification of this assumption.

Around 3.6–3.9 kyr ago, the anastomosing system was transformed back into a meander system (**Fig. 6**). At this stage of the research, pinpointing the precise cause for this shift is challenging. It is presumed, however, that climatic fluctuations during that period led to slightly higher amplitudes of annual flows in the Prosna River. This, in turn, triggered a return to more energetic river flows and the subsequent formation of point bars within a single-channel system. Given the relatively diminutive size and limited preservation of the point bars from this era, it can be conjectured that the development of the meanders was disrupted, potentially resulting in a reversion to a multi-channel (anastomosing) river system (see Kaniecki, 2011). This hypothesis is substantiated by an examination of archival topographic maps, revealing that as recently as 400 years ago, the Prosna River exhibited a multi-channel pattern (as noted by Małecki and Ptak, 2015). Substantive alterations to the river's pattern did not manifest until the 19th and 20th centuries.

6. Conclusions

The studies of the lower Prosna River valley infill gave an insight into evolution of extraglacial fluvial systems in Poland in the Late Glacial–Holocene period. On its basis we can reveal the following conclusions:

- The aggradation of deposits in the Prosna River valley likely occurred until the onset of the Late Glacial period. Preserved sediments on terrace IV suggest a predominant braided river style of sedimentation during this phase. Following this, the river incised into its bedrock, reaching a depth of 9–10 m.
- After a period of subdued erosion, large meanders emerged, albeit somewhat later compared with other river systems in the Polish Lowlands, occurring approximately 1000 years later. The analysed great meander displayed an unusual upstream rotation with a contraction, influenced by the slope direction of the resistant sub-Quaternary surface.
- A period of great meandering was followed by a relatively long period (8–10 kyr) of stabilisation in the valley and the development of an anastomosing system with slow aggradation, mainly of overbank facies.
- Around 3.6–3.9 kyr ago, the anastomosing system was transformed back into a meander system. The anastomosing system underwent a transformation back into a meander system. These meanders formed through simple expansion perpendicular to the valley's main axis.

However, they were significantly smaller than the great meanders of the Late Glacial period, with the entire episode lasting no more than 600–900 years.

- The period of small meanders, the Prosna River reverted to a multi-channel system. This configuration persisted until the 19th and 20th centuries when the river underwent regulation, in which it was incised into the bedrock by approximately 4 m, returning to a single-channel model.

Acknowledgements

References

Aitken MJ, 1998. *An Introduction to Optical Dating.* Oxford University Press, Oxford: 267 pp.

Berger GW, 2010. An alternate form of probability- distribution plot for De values. *Ancient TL 28*: 11–22.

Blum MD and Tornqvist TE, 2000. Fluvial response to climate and sea-level change: A review and look forward. *Sedimentology 47*: 2–48.

Bohncke S, Kasse C and Vandenberghe J, 1995. Climate induced environmental changes during the Vistulian Lateglacial at Żabinko, Poland. *Quaestiones Geographicae*, Special Issue *4*: 43–64.

Bridge JS and Demicco R, 2008. *Earth Surface Processes, Landforms and Sediment Deposits*. Cambridge University Press, Cambridge: 1–815.

Busschers FS, Weerts HJT, Wallinga J, Kasse C, Cleveringa P, De Wolf H and Cohen KM, 2005. Sedimentary architecture and optical dating of middle and Late Pleistocene Rhine-Meuse deposits – fluvial response to climate change, sea-level fluctuation and glaciation. *Netherlands Journal of Geosciences 84*: 25–41.

Folk RL and Ward WC, 1957. Brazos river bar: A study in the significance of grain size parameters. *Journal of Sedimentary Petrology 27*: 3–26.

Gabris G and Nador A, 2007. Long-term fluvial archives in Hungary: Response of the Danube and Tisza rivers to tectonic movements and climatic changes during the Quaternary: A review and synthesis. *Quaternary Science Reviews 26*: 2758–2782.

Galbraith R, Roberts R, Laslett G, Yoshida H and Olley J, 1999. Optical dating of single and multiple grains of quartz from Jinmium Rock Shelter, Northern Australia: Part I. Experimental design and statistical models. *Journal of Archaeometry 41*: 339–364. DOI 10.1111/j.1475-4754.1999.tb00988.x.

Gałka M, Lewandowska A, Niedzielski P, Sim TG, Swindles GT and Szczurek G, 2020. Late Glacial and early Holocene development of an oxbow lake in Central Europe (Poland) based on plant macrofossil and geochemical data. *The Holocene 30*(1): 178–189. DOI 10.1177/0959683619875803

Galloway WE and Hobday DK, 1996. Fluvial Systems In: *Terrigenous Clastic Depositional Systems*. Springer, Berlin, Heindelberg: p. 60–90, DOI 100.1007/978-3-642-61018-9_4.

Gębica P, Michczyńska DJ and Starkel L, 2015. Fluvial history of the Sub-Carpathian Basins (Poland) during the last cold stage (60–8 cal ka BP). *Quaternary International 388*: 119–141.

Ghazi F and Mountney NP, 2009. Facies and architectural element analysis of a meandering fluvial succession: The Permian Warchha Sandstone, Slat Range, Pakistan. *Sedimentary Geology 221*: 88–126.

Ghinassi M, Nemec W, Aldinucci M, Nehyba S, Özaksoy V and Fidolini F, 2014. Plan-form evolution of ancient meandering rivers reconstructed from longitudinal outcrop sections. *Sedimentology 61*: 952–977. DOI 10.1111/sed.12081.

Huisink M, 1997. Late-Glacial sedimentological and morphological changes in a lowland river in response to climatic change: The Maas, Southern Netherlands. *Journal of Quaternary Science 12*: 209–223.

Kaniecki A, 1976. Dynamika rzeki w świetle osadów trzech wybranych odcinków Prosny. Prace Komisji Geograficzno-Geologicznej - Poznańskie Towarzystwo Przyjaciół Nauk. PWN, Warszawa- Poznań.

Kaniecki A, 2011. Przemiany stosunków wodnych w dolinie górnej Noteci do połowy XIX wieku związane z antropopresją. Badania Fizjograficzne R. II – Seria A – *Geografia Fizyczna A62*: 41–58.

Kasse C, Bohncke SJP, Vandenberghe J and Gabris G, 2010. Fluvial style changes during the Last Glacial–interglacial transition in the middle Tisza valley (Hungary). *Proceedings of the Geologists' Association 121*: 180–194.

Kasse C, Hoek WZ, Bohncke SJP, Konert M, Weijers JWH, Cassee ML and Van der Zee RM, 2005. Late Glacial fluvial response of the Niers-Rhine (western Germany) to climate and vegetation change. *Journal of Quaternary Science 20*: 377–394. DOI 10.1002/jqs.923.

Kasse C, Vanderberghe J, Van Huissteden J, Bohncke SJP and Bos JAA, 2003. Sensitivity of Weichselian fluvial systems to climate change (Nochten mine, eastern Germany). *Quaternary Science Reviews 22*: 2141–2156.

Kleinhans MG and van den Berg JH, 2011. River channel and bar patterns explained and predicted by an empirical and a physics-based method. *Earth Surface Processes and Landforms 36*: 721–738.

Kozarski S, 1991. Warta- a case study of a lowland river. In: Starkel L, Gregory KJ and Thornes JB, eds., *Temperate Palaeohydrology*. Wiley, New York: 189–215.

Kozarski S, Gonera P and Antczak B, 1988. Valley floor development and paleohydrological changes: the Late Vistulian and Holocene history of the Warta River (Poland). In: Lang G and Schluchter C, eds, *Lake, Mire and River Environments During the Last 15 000 Years*. Balkema, Rotterdam: 185–203.

Kreutzer S, Burow C, Dietze M, Fuchs M, Schmidt C, Fischer M, Friedrich J, Riedesel S, Autzen M and Mittelstrass D, 2020. *Luminescence: Comprehensive Luminescence Dating Data Analysis*. R package version 0.9.10. WEB site: <https://CRAN.R-project.org/package=Luminescence>. Accessed 2021 July 28.

Lin Z, Wang C, Shan J, Han Z and Chen L, 2021. Reconstruction of meander-bend migration from associated channel-belt architecture recorded in successions of ancient meandering rivers: A case study from the Cretaceous Songliao Basin, China. *The Depositional Record 7*(3): 416–450.

Małecki ZJ and Ptak M, 2015. Zmiany biegu rzeki Prosny od Kalisza do jej ujścia. *Zeszyty Naukowe. Inżynieria Lądowa i Wodna w Kształtowaniu Środowiska,* Kalisz 13 (12) 61–72.

Marks L, Dzierżek J, Janiszewski R, Kaczorowski J, Lindner L, Majecka A, Makos M, Szymanek M, Tołoczko-Pasek A and Woronko B, 2016. Quaternary stratigraphy and palaeogeography of Poland. *Acta Geologica Polonica 66*: 410–434. DOI 10.1515/agp-2016-0018.

Miall AD, 1978. Lithofacies types and vertical profile models in braided rivers: A summary. In: Miall AD, ed., *Fluvial Sedimentology*. *Canadian Society of Petroleum Geologists, Memoir 5* Canadian Society of Petroleum Geologists, Calgary,: 597–604.

Miall AD, 2006. The Geology of Fluvial Deposits: Sedimentary Facies, Basin Analysis and Petroleum Geology, 4th ed. Springer, Berlin, Heidelberg, New York: 1–582.

Miall AD, 2014. *Fluvial Depositional Systems*. Springer, New York: pp. 1–316.

Mol J, Vandenberghe J and Kasse C, 2000. River response to variations of periglacial climate in mid-latitude Europe. *Geomorphology 33*: 131–148.

Moska P, 2019. Luminescence dating of Quaternary sediments – some practical aspects. *Studia Quaternaria 36*: 2161–169.

Moska P, Bluszcz A, Poręba G, Tudyka K, Adamiec G, Szymak A and Przybyła A, 2021. Luminescence dating procedures at the Gliwice luminescence dating laboratory. *Geochronometria 48*: 1–15. DOI 10.2478/geochr-2021-0001.

Moska P, Sokołowski RJ, Jary Z, Zieliński P, Raczyk J, Szymak A, Krawczyk M, Skurzyński J, Poręba G, Łopuch M and Tudyka K, 2022. Stratigraphy of the Late Glacial and holocene aeolian series in different sedimentary zones related to the Last Glacial maximum in Poland. *Quaternary International 630*: 65–83. DOI 10.1016/j.quaint.2021.04.004.

Moska P, Sokołowski RJ, Zieliński P, Jary Z, Raczyk J, Mroczek P, Szymak A, Krawczyk M, Skurzyński J, Poręba G, Łopuch M and Tudyka K, 2023. An impact of short-term climate oscillations in the Late Pleniglacial and Late Glacial on sedimentary processes and the pedogenic record in central Poland. *Annals of the American Association of Geographers 113*: 46–70. DOI 10.1080/24694452.2022.2094325.

Murray AS and Wintle AG, 2000. Luminescence dating of quartz using an improved single-aliquot regenerative-dose protocol. *Radiation Measurements 32*: 57–73. DOI 10.1016/S1350-4487(99)00253-X.

Nanson GC and Hickin EJ, 1983. Channel migration and incision on the Beatton River. *Journal of Hydraulic Engineering 109*(3): 327–337.

Newman DR, Lindsay JB and Cockburn JMH, 2018. Evaluating metrics of local topographic position for multiscale geomorphometric analysis. *Geomorphology 312*: 40–50. DOI 10.1016/j.geomorph.2018.04.003.

Panin A and Matlakhova E, 2015. Fluvial chronology in the east European plain over the last 20 ka and its palaeohydrological implications. *Catena 130*: 46–61. DOI 10.1016/j.catena.2014.08.016.

Parker G and Andrews ED, 1986. On the time development of meander bends. *Journal of Fluid Mechanics 162*(-1): 139–156. DOI 10.1017/s0022112086001970

Peeters J, Busschers FS, Stouthamer E, Bosch JHA, Van den Berg MW, Wallinga J, Versendaal AJ, Bunnik FPM and Middelkoop H, 2016. Sedimentary architecture and chronostratigraphy of a late Quaternary incised-valley fill: A case study of the late middle and Late Pleistocene Rhine system in the Netherlands. *Quaternary Science Reviews 131*: 211–236.

Pisarska-Jamroży M and Weckwerth P, 2013. Soft-sediment deformation structures in a Pleistocene glaciolacustrine delta and their implications for the recognition of subenvironments in delta deposits. *Sedimentology 60*: 637–665.

Pożaryski W and Kalicki T, 1995. Evolution of gap section of the Vistula valley in the Lateglacial and Holocene. In: Starkel L, ed., *Evolution of the Vistula River valley during the last 15000 years, part V*. Geographical Studies Special Issue, Wrocław 8 (IGiPZ PAN): 111–137.

Przedwojski B, 2006. Morfologia Koryt Rzecznych, Pomiary, Prognozowanie i modelowanie Procesów Rzecznych. *Infrastruktura i Ekologia Terenów Wiejskich 4*: 101–129.

Rotnicki K and Borówka RK, 1990. New data on the age of the maximum advance of the Vistulian ice sheet during the Leszno Phase. *Quaternary Studies in Poland 9*: 73–83.

Rotnicki K and Latałowa M, 1986. Palaeohydrology and fossilization of a meandering channel of Younger Dryas age in the middle Prosna river valley. *Quaternary Studies in Poland 7*: 73–90.

Rotnicki K and Młynarczyk Z, 1998. Late Vistulian and Holocene channel forms and deposits of the middle Prosna River and their palaeohydrological interpretation. *Quaestiones Geographicae 13/14*: 113–162.

Rotnicki K, 1987. Main phases of erosion and accumulation in the middle and lower Prosna valley in the last glacial-interglacial cycle. *Geographia Polonica 53*: 53–65.

Rotnicki K, Rotnicka J and Młynarczyk Z, 2005. Szczegółowa Mapa Geologiczna Polski w Skali 1:50 000, arkusz Trąbczyn wraz z objaśnieniami. [Detailed Geological Map of Poland, 1:50000, sheet Trąbczyn with explanation]. Polish Geological Institute, Warsaw (in Polish).

Rząsa S and Owczarzak W, 2013. Methods for the Granulometric Analysis of Soils for Science and Practice. *Polish Journal of Soil and Science* 46(1).

Sidorchuk A, Borisova O and Panin A, 2001. Fluvial response to the Late Valdai/Holocene environmental change on the East European Plain. *Global and Planetary Change 28*: 303–310.

Sokołowski RJ, Molodkov A, Hrynowiecka A, Woronko B and Zieliński P, 2021. The role of an ice-sheet, glacioisostatic movements and climate in the transformation of Middle Pleistocene depositional systems: A case study from the Reda site, northern Poland. *Geografiska Annaler: Series A, Physical Geography 103*(3): 223–258. DOI 10.1080/04353676.2021.1926241.

Sørensen R, Zinko U and Seibert J, 2006. On the calculation of the topographic wetness index: evaluation of different methods based on field observations. *Hydrology and Earth System Sciences 10*: 101–112.

Starkel L, Gębica P and Superson J, 2007. Last Glacial–Interglacial cycle in the evolution of river valleys in southern and central Poland. *Quaternary Science Review 26*: 22–24: 2924–2936. DOI 10.1016/j.quascirev.2006.01.038.

Starkel L, Michczyńska DJ, Gębica P, Kiss T, Panin A and Persoiu I, 2015. Climatic fluctuations reflected in the evolution of fluvial systems of Central-Eastern Europe (60-8 ka cal BP). *Quaternary International 388*: 97–118. DOI 10.1016/j.quaint.2015.04.017

Szałamacha G, 1999. Szczegółowa Mapa Geologiczna Polski w skali 1:50 000, Ark. Pleszew [Detailed Geological Map of Poland, 1:50000, sheet Pleszew]. Polish Geological Institute, Warsaw (in Polish).

Tudyka K, Koruszowic M, Osadnik R, Adamiec G, Moska P, Szymak A, Bluszcz A, Zhang J, Kolb T and Poręba G, 2023. µRate: An online dose rate calculator for trapped charge dating. *Archaeometry 65*: 423–443. DOI 10.1111/arcm.12828.

Van Huissteden J and Kasse C, 2001. Detection of rapid climate change in Last Glacial fluvial successions in The Netherlands. *Global and Planetary Change 28*: 319–339

Vandenberghe J and Sidorchuk A, 2020. Large Palaeomeanders in Europe: Distribution, Formation Process, Age, Environments and Significance. *In: Palaeohydrology*: 169–186. DOI 10.1007/978-3-030-23315-0_9

Vandenberghe J, 2008. The fluvial cycle at cold-warm-cold transitions in lowland regions: A refinement of theory. *Geomorphology 98*: 275–284.

Vandenberghe J, 2015. River terraces as a response to climatic forcing: formation processes, sedimentary characteristics and sites for human occupation. *Quaternary International 370*: 3–11.

Vandenberghe J, Kasse C, Bohncke SJP and Kozarski S, 1994. Climate-related river activity at the Weichselian–Holocene transition: A comparative study of the Warta and Maas rivers. *Terra Nova 6*: 476–485.

Weiss AD, 2001. Topographic position and landforms analysis. In: *Poster Presentation, ESRI Users Conference*, San Diego, CA.

Zieliński P, Sokołowski RJ, Jankowski M, Standzikowski K and Fedorowicz S, 2019. The climatic control of sedimentary environment changes during the Weichselian–An example from the Middle Vistula Region (eastern Poland). *Quaternary International 501*: 120–134.

Zieliński T, 2014. Sedimentologia. Osady rzek i jezior [Sedimentology. Deposits of Rivers and Lakes]. Wydawnictwo Naukowe UAM, Poznań: 1–594 (in Polish)